nature climate change

LETTERS

https://doi.org/10.1038/s41558-020-0693-4

There are amendments to this paper

Reduced European aerosol emissions suppress winter extremes over northern Eurasia

Yuan Wang[1,2*], Tianhao Le[1], Gang Chen[3], Yuk L. Yung[1,2], Hui Su[2], John H. Seinfeld[4] and Jonathan H. Jiang[2*]

Winter extreme weather events receive major public attention due to their serious impacts[1], but the dominant factors regulating their interdecadal trends have not been clearly established[2,3]. Here, we show that the radiative forcing due to geospatially redistributed anthropogenic aerosols mainly determined the spatial variations of winter extreme weather in the Northern Hemisphere during 1970–2005, a unique transition period for global aerosol forcing[4]. Over this period, the local Rossby wave activity and extreme events (top 10% in wave amplitude) exhibited marked declining trends at high latitudes, mainly in northern Eurasia. The combination of long-term observational data and a state-of-the-art climate model revealed the unambiguous signature of anthropogenic aerosols on the wintertime jet stream, planetary wave activity and surface temperature variability on interdecadal timescales. In particular, warming due to aerosol reductions in Europe enhanced the meridional temperature gradient on the jet's poleward flank and strengthened the zonal wind, resulting in significant suppression in extreme events over northern Eurasia. These results exemplify how aerosol forcing can impact large-scale extratropical atmospheric dynamics, and illustrate the importance of anthropogenic aerosols and their spatiotemporal variability in assessing the drivers of extreme weather in historical and future climate.

Wintertime extreme cold temperatures, frost and blizzards impact many people living in the mid-latitudes, especially the Northern Hemisphere. However, an understanding of the decadal and interdecadal trends of winter extreme events remains elusive, as trend assessments are sensitive to the region of study and time period analysed[1–3]. More fundamentally, the lack of consensus on changes in winter extreme weather stems from the intrinsic complexity of mid-latitude weather systems and rapidly changing environmental factors, as well as internal climate system variability, such as the Northern Annular Mode[5]. The role of anthropogenic forcing in winter extremes is also uncertain, as the dynamical response is multifaceted and nonlinear[6]. For example, a warmer climate characterized by polar amplification is hypothesized to reduce the meridional temperature gradient and result in a slower but more complex mid-latitude jet stream[7,8]. Moreover, the tropical expansion of the Hadley cell in response to global warming can shift the jet stream poleward and counteract the influence of Arctic sea ice loss[9], forming a 'tug-of-war'[10].

As the second-largest climate forcer in the Earth system, atmospheric aerosols (mainly attributed to urbanization and industrialization) have been closely linked to climate change in both the mean state and extreme events[11–13]. Anthropogenic aerosols can exert a radiative cooling of about $-0.8\,\mathrm{W\,m^{-2}}$ globally[14], by both directly scattering solar radiation back to space and indirectly brightening shallow clouds via the cloud condensation nuclei effect. The spatial heterogeneity of anthropogenic aerosol emissions causes them to have highly regional impacts, and previous research has found that they can weaken the South and East Asian monsoons[15,16], modulate the Pacific storm track[17] and impact twentieth-century North Atlantic climate variability[18]. Anthropogenic aerosols that absorb solar radiation, such as black carbon, contributed to the recent tropical expansion in the Northern Hemisphere by inducing atmospheric heating and altering thermodynamic profiles[19]. Furthermore, anthropogenic aerosol emissions have exhibited regional changes on decadal timescales, with a shift from developed to developing countries since the 1970s[4]. Consequently, a positive radiative forcing has emerged from the reduction in anthropogenic aerosols across Europe and North America, along with a strong negative radiative forcing in China and India linked to aerosol increases. This 'see-saw' radiative forcing pattern imprinted on regional surface temperature and tropical precipitation[19] and interfered with the pace of Arctic sea ice melt[20]. Here, we aim to unravel the extent to which this pattern modulates wintertime extreme weather events via its influence on the large-scale atmospheric circulation and mid-latitude dynamics.

We examined variations of winter extreme events using the local Rossby wave activity (LWA) index, which quantifies the frequency and intensity of synoptic weather systems in mid-latitudes[21] (Methods and Supplementary Text 1). A larger LWA indicates more severe weather events—typically either extratropical cyclones or blocking anticyclones. The observed long-term wintertime LWA trends were derived based on six-hourly geopotential height at 500 hPa from a reanalysis dataset. A spatial map of LWA trends during 1970–2005 (Fig. 1a) shows spatial variation of winter weather systems superimposed on an overall declining trend. The major reductions in LWA occurred in northern Eurasia and eastern Canada[22]. Synoptic weather systems over western Europe, western Canada and the northwest Pacific became more frequent during 1970–2005. Decomposing the LWA into cyclonic and anticyclonic events shows that positive LWA trends near the west coasts of Eurasia and North America are coincident with anticyclones, while those near the east coasts are linked to cyclones (Supplementary Fig. 1). Zonal mean LWA trends show a significant decline with a maximum near 65° N, but no significant change over the latitudes south

[1]Division of Geological and Planetary Sciences, California Institute of Technology, Pasadena, CA, USA. [2]Jet Propulsion Laboratory, California Institute of Technology, Pasadena, CA, USA. [3]Department of Atmospheric and Oceanic Sciences, University of California, Los Angeles, CA, USA. [4]Divisions of Chemistry and Chemical Engineering and Engineering and Applied Science, California Institute of Technology, Pasadena, CA, USA.
*e-mail: yuan.wang@caltech.edu; jonathan.h.jiang@jpl.nasa.gov

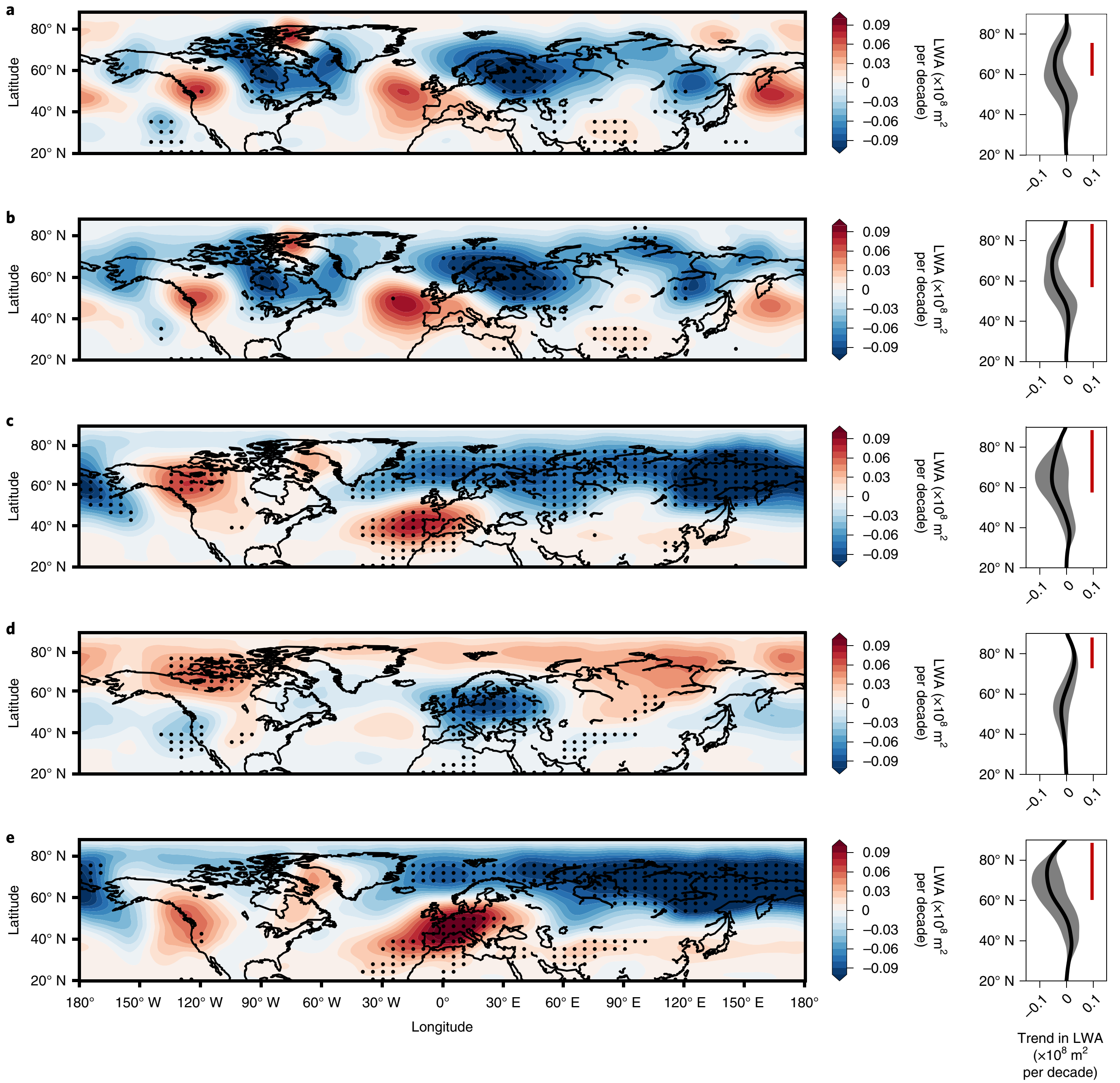

Fig. 1 | LWA trends from reanalysis and model simulation over December to February during 1970–2005. a–e, Spatial patterns of LWA trends (left column) and their zonal mean distribution (right column) for: JRA55 (**a**); JRA55 with removal of trends in major known climate oscillation indices (**b**); CESM ALL results (**c**); CESM NO_AERO results (**d**); and CESM ALL – NO_AERO (DIFF) (**e**). Black dots (each representing 16 grid points) indicate that the local linear trend is significant at the 90% confidence level using a Student's *t*-test and the field significance test[28]. Shading in the zonal mean plots indicates spread of the LWA trend at the same latitude. The red vertical bars denote latitude zones with significant LWA trends (shades do not overlap with the 0 m^2 per decade line).

of 50° N. As a result, the Northern Hemisphere LWA mean does not exhibit a significant trend during 1970–2005. Jet stream sinuosity—an independent index for mid-latitude extreme weather—confirms this (Supplementary Text 2 and Supplementary Fig. 2). In this period, there was global warming of about +0.12 °C per decade surface temperature increase. Thus, the existing theory that enhanced jet stream sinuosity and LWA follow polar amplification is not capable of explaining such an interdecadal trend, indicating that other factors are at play. To better characterize extreme weather variability, we also examined the top 10% of events measured by wave amplitude of wintertime LWA, and we quantified these trends (Supplementary Fig. 3). The resulting spatial patterns closely resemble seasonal mean LWA trends, showing a consistent and significant reduction over northern Eurasia.

To minimize the influence of internal ocean and atmosphere variability on the decadal trend detected above, we performed a

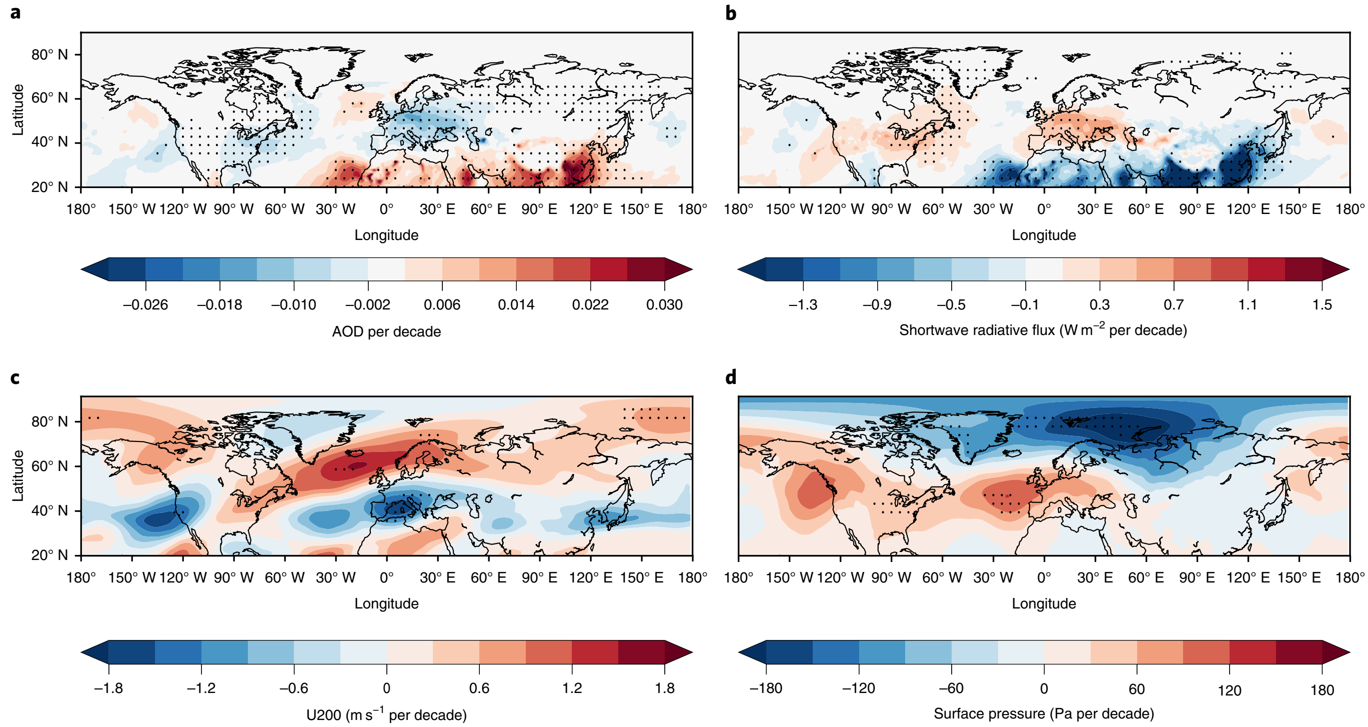

Fig. 2 | CESM wintertime changes from 1970–2005 (DIFF). a, AOD. **b**, Shortwave radiative flux at the surface in clear sky. **c**, U200. **d**, Surface pressure. Black dots (each representing 16 grid points) indicate that the local linear trend is significant at the 90% confidence level using a Student's *t*-test and the field significance test.

multivariate linear regression of LWA on five climate indices (equation (2)). We find that the broad-scale LWA trends still hold after this step, with northern Eurasia and the North Atlantic experiencing increased statistical significance (Fig. 1b). Similarly, the declining trends of LWA extremes over northern Eurasia remain robust (Supplementary Fig. 3). Moreover, the trends based on reanalysis data are robust even with an analysis period starting from 1979—the beginning of the satellite era.

To further attribute the LWA trends in the reanalysis product, we performed transient forcing sensitivity simulations using a fully coupled global climate model with a comprehensive representation of radiative forcing in the Earth system. This model reproduces geopotential height and LWA climatologies well compared with reanalysis data (Supplementary Fig. 4). We assessed the influence of anthropogenic aerosol changes since the 1970s using two groups of ensemble simulations during 1970–2005—one with all forcings (ALL) and another with all but anthropogenic aerosols (NO_AERO). The differences (DIFF) between those two groups qualitatively reflect the importance of the aerosol effects. The simulation group under each emission scenario consists of three ensemble members for statistical significance. ALL simulations show similar trends for winter LWA in the Northern Hemisphere (Fig. 1c). This confirms the fidelity of the Community Earth System Model (CESM) in reproducing historical climate. In contrast, NO_AERO exhibits patterns distinct from ALL and the reanalysis product over most regions except eastern Europe (Fig. 1d). The spatial patterns in DIFF largely resemble those in ALL (Fig. 1e). The resemblance of these patterns among reanalysis, ALL and DIFF indicates that anthropogenic aerosols are a dominant driver of changes in winter wave events over Eurasia during 1970–2005.

More details on the role of anthropogenic aerosols are revealed in CESM sensitivity simulations. The changes in anthropogenic aerosol burden in the atmosphere (Fig. 2a) and related radiative forcing (Fig. 2b) are confined largely to the aerosol source regions: aerosol reduction and associated warming in Europe and the United States; and aerosol elevation and associated cooling in East and South Asia. Nevertheless, the influence of anthropogenic aerosols can propagate worldwide through large-scale atmosphere and ocean feedbacks. With respect to extreme weather, the most relevant changes lie in the altered jet stream strength and location. This is evidenced by the zonal wind at 200 hPa (U200), which is reduced near 40° N but significantly enhanced over 60° N (Fig. 2c). The maximum reduction at 40° N is about 10% per decade. Such a poleward shift of the jet results in a smaller latitude range of the jet, reducing its likelihood of extending southward in the form of cold air outbreaks, and explaining the overall reduction of LWA in the Northern Hemisphere winter. Regionally, the most prominent change in the jet stream occurs as a sharp contrast between southern and northern Europe. By comparison with the aerosol forcing pattern (Fig. 2b), warming resulting from aerosol reductions in Europe enhances the meridional temperature gradient on the jet's poleward flank. This enhancement reduces the equatorward gradient, consequently strengthening the zonal wind to the north and weakening it to the south.

We also note that the signs of U200 trends are generally the opposite of those of LWA for most regions, lending support to the idea that a less wavy jet stream leads to less weather variability[23]. Surface pressure shows negative anomalies over the Arctic (Fig. 2d) under aerosol forcing. Together with the U200 and sinuosity changes, surface pressure patterns largely resemble a positive phase of the Arctic Oscillation. We do not find significant changes in sea ice over the entire Arctic in DIFF (Supplementary Fig. 5), consistent with previous work on the muted response of sea ice to anthropogenic aerosol variations[20]. Hence, the observed and simulated changes in LWA during this period are probably not explained by the forcings and/or feedbacks in the Arctic[24].

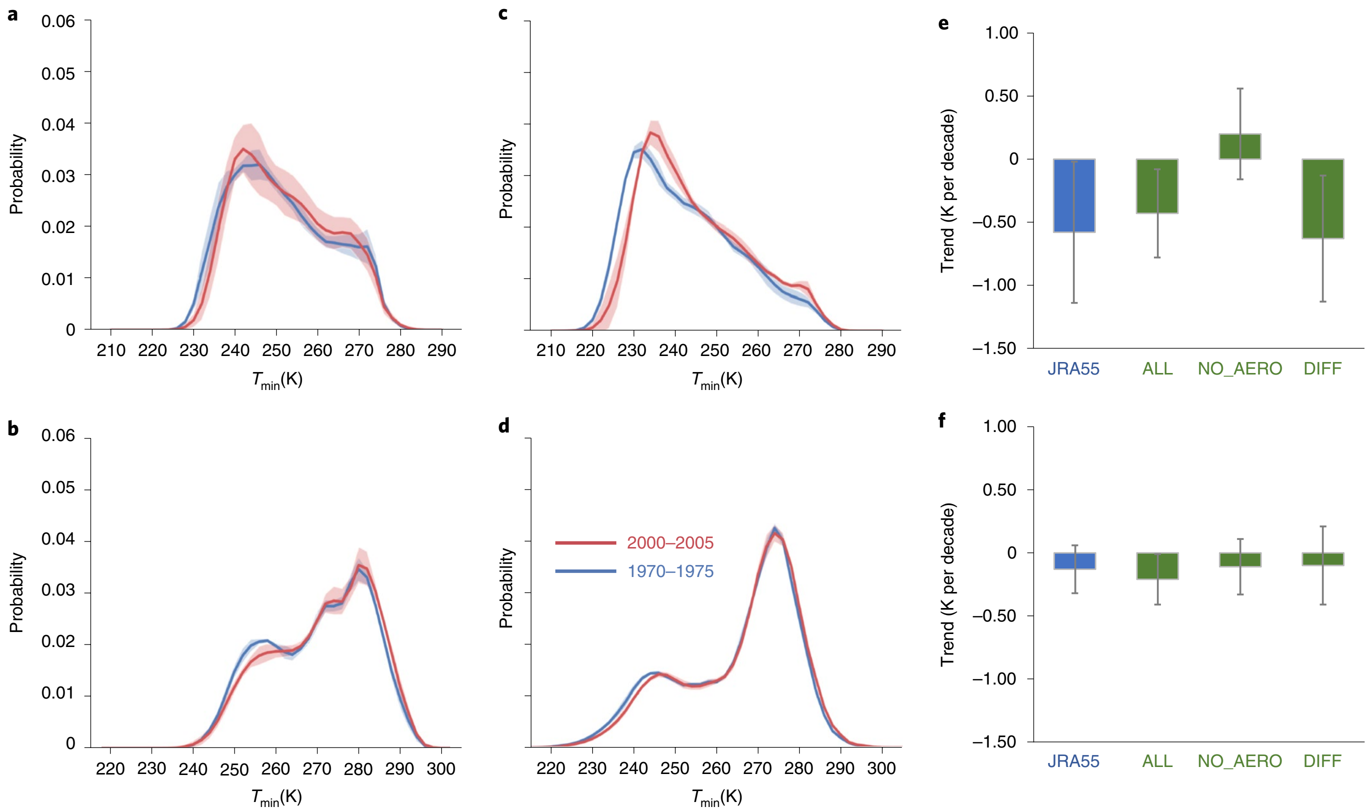

Fig. 3 | Observed and simulated variations in December to February T_{min} over Eurasia (0–150° E, 20–80° N). a–d, PDF of wintertime T_{min} (as determined by JRA55 (**a** and **b**) or CESM ALL (**c** and **d**)), averaged over two periods (1970–1975 (blue) and 2000–2005 (red)), for two latitude zones (50–80° N (**a** and **c**) and 20–50° N (**b** and **d**)). **e**,**f**, Difference between the 5th and 95th percentile of T_{min} and its decadal trend, in JRA55 and the three CESM emission scenarios, for 50–80° N (**e**) and 20–50° N (**f**). Shading in the PDFs denotes the spread (1 s.d.) among different years in each period. The error bars in **e** and **f** denote the 95% confidence intervals for each trend analysis. The distributions of T_{min} are significantly different between the two time periods in **a** and **c** according to the two-sample Kolmogorov–Smirnov test ($P < 0.01$).

Anthropogenic impacts on winter extreme cold temperature can emerge via changes in local surface radiation fluxes and variations in heat and moisture transport by altered large-scale circulations and wave activity. In addition, the relationship between jet stream variability and surface temperature change exhibits strong regional dependency[25], so we focus on the response of winter surface temperature extremes over Eurasia, which shows the most significant trends in LWA. The probability distribution function (PDF) of daily minimum land-surface temperature (T_{min}) in the reanalysis shows an overall shift of winter T_{min} occurrence from low to high temperature between 50° and 80° N (Fig. 3a), consistent with a global warming trend in wintertime mean temperature during 1970–2005. With respect to the extremes, the significant right shift of the PDF's left tail (from the blue to the red line in Fig. 3a) indicates a reduction of extreme cold days and an increase in annual coldest temperature in Eurasia in 2000–2005 compared with 1970–1975. The T_{min} PDFs from CESM ALL simulations resemble the PDFs from the reanalysis and, more importantly, reproduce the shift within the 35-year period (Fig. 3c). Note that the NO_AERO simulations also reproduce a similar PDF shift (Supplementary Fig. 6), further supporting the dominant role of greenhouse gases in reducing the coldest days of the year. The PDFs from a lower latitude zone (20–50° N) show a much weaker shift in temperature PDF in both reanalysis and the model (Fig. 3b,d).

In addition to the occurrence frequency of the coldest temperature, the day-to-day temperature fluctuations within a season are also of interest. These fluctuations can be quantified by the difference of T_{min} between the top fifth percentile (averaged over the hottest days) and the bottom fifth percentile (averaged over the coldest days)[26,27]. The temperature fluctuations are dampened due to less wave activity between 50° and 80° N (Fig. 3e). Such a reduction in temperature range is reproduced only in the ALL and DIFF experiments, corroborating our previous finding that anthropogenic aerosols, rather than greenhouse gases, play the decisive role in changing surface temperature variation ranges, following the alteration of wave activities. Temperature fluctuation does not show a significant trend over 20–50° N in either the reanalysis data or the model simulations (Fig. 3f).

The magnitude of future anthropogenic aerosol reductions in Europe and the United States is anticipated to be much smaller than that during 1970–2005, owing to legislation aimed at reducing anthropogenic aerosols and their precursor gases. Additionally, anthropogenic aerosols in China are projected to decrease by up to 85% before 2050[20]. The map of future aerosol optical depth (AOD) changes clearly shows that major aerosol reductions will occur over eastern China in the next three decades (Fig. 4a). Following such an east-heavy aerosol forcing pattern, LWA is mainly reduced over northeast Eurasia, leaving Central or West Eurasia largely unchanged (Fig. 4b). Similar to the historical simulations, mid-latitude aerosol reductions induce an enhancement of the jet at its poleward flank (Fig. 4c).

The present study focuses on the anthropogenic effects on mean state changes in climate and circulation as well as weather extremes, as exemplified by wave activity and surface temperature extremes. As opposed to previous studies of greenhouse gas forcing and its consequences on Arctic amplification[6,8,23,26], here we provide a

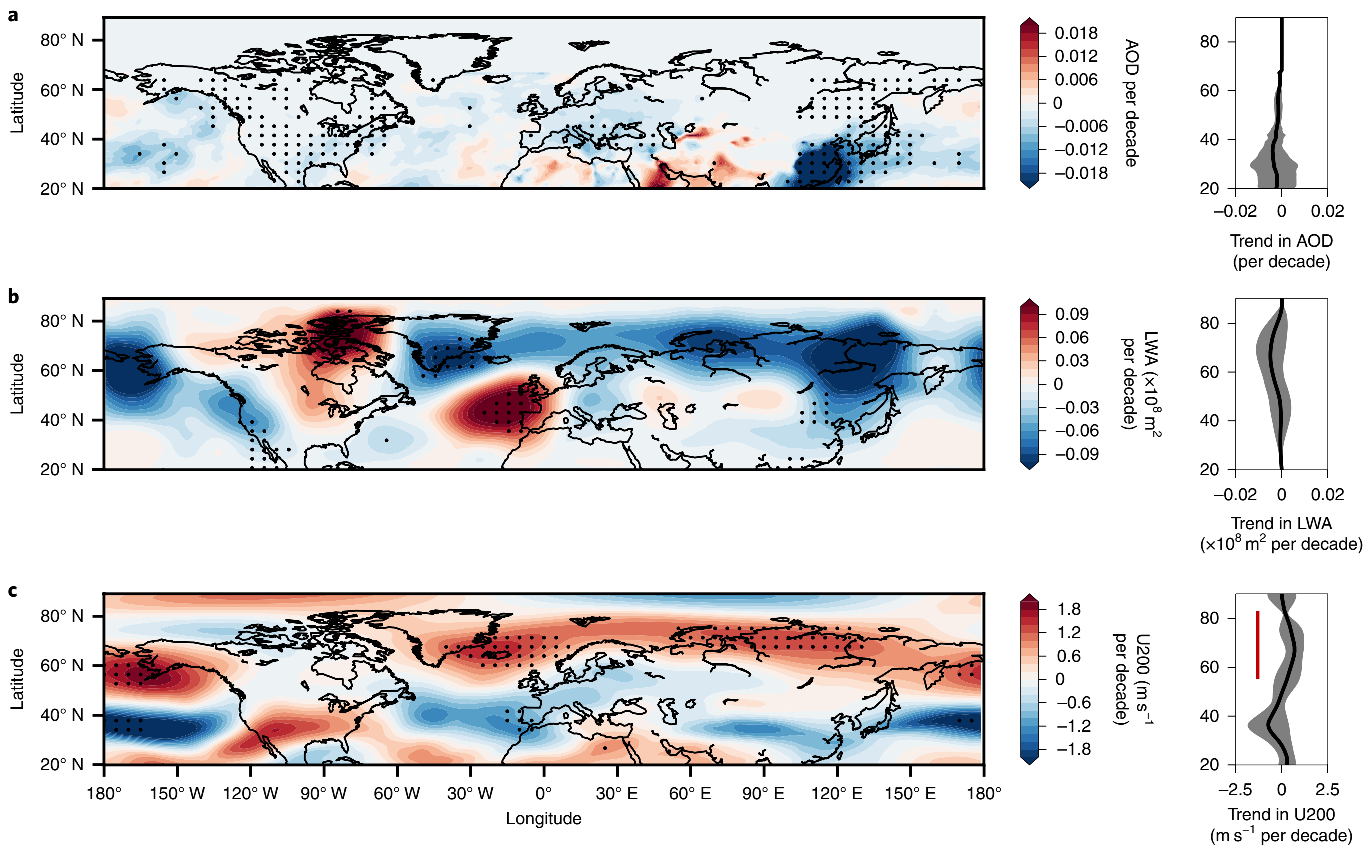

Fig. 4 | CESM future wintertime changes in DIFF during 2015–2045. a, AOD. **b**, LWA. **c**, U200. Black dots (each representing 16 grid points) indicate that the local linear trend is significant at the 90% confidence level using a Student's *t*-test and the field significance test. The red vertical bars denote latitude zones with significant trends (shades do not overlap with the lines representing 0 on the *x* axis).

different perspective on spatially heterogeneous aerosol forcing when explaining trends of winter weather extremes.

Online content

Any methods, additional references, Nature Research reporting summaries, source data, extended data, supplementary information, acknowledgements, peer review information; details of author contributions and competing interests; and statements of data and code availability are available at https://doi.org/10.1038/s41558-020-0693-4.

Received: 12 July 2019; Accepted: 7 January 2020;
Published online: 3 February 2020

References

1. Cohen, J., Pfeiffer, K. & Francis, J. A. Warm Arctic episodes linked with increased frequency of extreme winter weather in the United States. *Nat. Commun.* **9**, 869 (2018).
2. Sun, L., Perlwitz, J. & Hoerling, M. What caused the recent "Warm Arctic, Cold Continents" trend pattern in winter temperatures? *Geophys. Res. Lett.* **43**, 5345–5352 (2016).
3. Barnes, E. A., Dunn-Sigouin, E., Masato, G. & Woollings, T. Exploring recent trends in Northern Hemisphere blocking. *Geophys. Res. Lett.* **41**, 638–644 (2014).
4. Wang, Y., Jiang, J. H. & Su, H. Atmospheric responses to the redistribution of anthropogenic aerosols. *J. Geophys. Res.* **120**, 9625–9641 (2015).
5. Scaife, A. A., Folland, C. K., Alexander, L. V., Moberg, A. & Knight, J. R. European climate extremes and the North Atlantic Oscillation. *J. Clim.* **21**, 72–83 (2008).
6. Schneider, T., Bischoff, T. & Płotka, H. Physics of changes in synoptic midlatitude temperature variability. *J. Clim.* **28**, 2312–2331 (2015).
7. Cohen, J. et al. Recent Arctic amplification and extreme mid-latitude weather. *Nat. Geosci.* **7**, 627–637 (2014).
8. Francis, J. A. & Vavrus, S. J.Evidence for a wavier jet stream in response to rapid Arctic warming. *Environ. Res. Lett.* **10**, 014005 (2015).
9. Seidel, D. J. et al. Widening of the tropical belt in a changing climate. *Nat. Geosci.* **1**, 21–24 (2008).
10. Screen, J. A. et al. Consistency and discrepancy in the atmospheric response to Arctic sea-ice loss across climate models. *Nat. Geosci.* **11**, 155–163 (2018).
11. Seinfeld, J. H. et al. Improving our fundamental understanding of the role of aerosol–cloud interactions in the climate system. *Proc. Natl Acad. Sci. USA* **113**, 5781–5790 (2016).
12. Fan, J., Wang, Y., Rosenfeld, D. & Liu, X. Review of aerosol–cloud interactions: mechanisms, significance, and challenges. *J. Atmos. Sci.* **73**, 4221–4252 (2016).
13. Guo, J. et al. Declining frequency of summertime local-scale precipitation over eastern China from 1970–2010 and its potential link to aerosols. *Geophys. Res. Lett.* **44**, 5700–5708 (2017).
14. IPCC *Climate Change 2013: The Physical Science Basis* (eds Stocker, T. et al.) (Cambridge Univ. Press, 2013).
15. Bollasina, M. A., Ming, Y. & Ramaswamy, V. Anthropogenic aerosols and the weakening of the South Asian summer monsoon. *Science* **334**, 502–505 (2011).
16. Li, Z. et al. Aerosol and monsoon climate interactions over Asia. *Rev. Geophys.* **54**, 866–929 (2016).
17. Wang, Y., Zhang, R. & Saravanan, R. Asian pollution climatically modulates mid-latitude cyclones following hierarchical modelling and observational analysis. *Nat. Commun.* **5**, 3098 (2014).
18. Booth, B. B., Dunstone, N. J., Halloran, P. R., Andrews, T. & Bellouin, N. Aerosols implicated as a prime driver of twentieth-century North Atlantic climate variability. *Nature* **484**, 228–232 (2012).
19. Allen, R. J., Sherwood, S. C., Norris, J. R. & Zender, C. S. Recent Northern Hemisphere tropical expansion primarily driven by black carbon and tropospheric ozone. *Nature* **485**, 350–354 (2012).

20. Wang, Y. et al. Elucidating the role of anthropogenic aerosols in arctic sea ice variations. *J. Clim.* **31**, 99–114 (2018).
21. Chen, G., Lu, J., Burrows, D. A. & Leung, L. R. Local finite-amplitude wave activity as an objective diagnostic of midlatitude extreme weather. *Geophys. Res. Lett.* **42**, 10952–10960 (2015).
22. Peings, Y., Cattiaux, J., Vavrus, S. & Magnusdottir, G. Late twenty-first-century changes in the midlatitude atmospheric circulation in the CESM large ensemble. *J. Clim.* **30**, 5943–5960 (2017).
23. Coumou, D., Lehmann, J. & Beckmann, J. The weakening summer circulation in the Northern Hemisphere mid-latitudes. *Science* **348**, 324–327 (2015).
24. Liu, J. P., Curry, J. A., Wang, H. J., Song, M. R. & Horton, R. M. Impact of declining Arctic sea ice on winter snowfall. *Proc. Natl Acad. Sci. USA* **109**, 4074–4079 (2012).
25. Röthlisberger, M., Pfahl, S. & Martius, O. Regional-scale jet waviness modulates the occurrence of midlatitude weather extremes. *Geophys. Res. Lett.* **43**, 10989–10997 (2016).
26. Rhines, A., McKinnon, K. A., Tingley, M. P. & Huybers, P. Seasonally resolved distributional trends of North American temperatures show contraction of winter variability. *J. Clim.* **30**, 1139–1157 (2017).
27. Martineau, P., Chen, G. & Burrows, D. A. Wave events: climatology, trends, and relationship to Northern Hemisphere winter blocking and weather extremes. *J. Clim.* **30**, 5675–5697 (2017).
28. Wilks, D. S. The stippling shows statistically significant grid points: how research results are routinely overstated and overinterpreted, and what to do about it. *Bull. Am. Meteorol. Soc.* **97**, 2263–2273 (2016).

Publisher's note Springer Nature remains neutral with regard to jurisdictional claims in published maps and institutional affiliations.

Methods

LWA calculation. We characterize the mid-latitude extreme weather events by quantifying the waviness of the westerly circulation based on six-hourly geopotential height at 500 hPa (Z_{500})[21]. This yields a daily two-dimensional map, as exemplified in Supplementary Fig. 7. The LWA of geopotential height at longitude λ and latitude ϕ is measured as:

$$\mathrm{LWA}(\lambda,\phi_e)=\frac{a}{\cos\phi_e}\left[\int_{\hat{z}\geq 0,\phi\geq\phi_e(Z_{500})}\hat{z}(\lambda,\phi)\cos\phi\,\mathrm{d}\phi - \int_{\hat{z}\leq 0,\phi\leq\phi_e(Z_{500})}\hat{z}(\lambda,\phi)\cos\phi\,\mathrm{d}\phi\right] \quad (1)$$

where λ is the longitude, a is the radius of Earth, z is the geopotential height and ϕ_e is the equivalent latitude after adjusting the height contour Z_{500} to the zonally symmetric basic state without any change to the encircled area by the Z_{500} contour. $\hat{z}(\lambda,\phi)=z(\lambda,\phi)-Z_{500}(\phi_{500})$ is an eddy term describing the deviation from the basic state. LWA represents the combination of the zonal amplitude $\hat{z}$ and meridional meandering of a planetary wave described in ref. [21].

Removing internal variability by multivariate linear regression. We apply a multivariate linear regression model to separate anthropogenic influence from possible internal variability on the trends of winter extreme weather. The model has the form:

$$\mathrm{LWA}=a\times\mathrm{AO}+b\times\mathrm{PDO}+c\times\mathrm{Strato}+d\times\mathrm{ENSO}+e\times\mathrm{QBO}+\mathrm{residuals} \quad (2)$$

where a–e are regression coefficients. The LWA values going into the regression are the winter means at each grid point in the Northern Hemisphere. Five climate indices are considered here, including the Arctic Oscillation (AO), Pacific Decadal Oscillation (PDO), stratosphere variability (Strato), El Niño–Southern Oscillation (ENSO) and Quasi-Biennial Oscillation (QBO). They are calculated over the boreal winter (December to February) of each year as well. Their correlations with LWA on the interannual time scale are shown in Supplementary Text 3. Rossby wave activity can be influenced by stratospheric variability (for example, ref. [29]), especially in the winter when the stratospheric polar vortex is strong. Hence, we derive an index (Strato) using the monthly mean zonal wind at 10 hPa and 60° N to account for such stratospheric variability. Trend analyses on the residuals from the regression are re-performed to explore the anthropogenic influence with minimized internal variability on the decadal scale. Considering that the AO and North Atlantic Oscillation (NAO) are often closely related (the NAO is often considered to be a regional expression of the AO), we do not include the NAO in the model.

Also note that anthropogenic aerosol forcing is known to impact some of this climate variability as well. General circulation models show that anthropogenic aerosol forcing since the 1990s projects onto the PDO and contributes to the recent global surface warming slowdown[30]. Hence, the LWA signals from this regression method could be smaller than the real anthropogenic forcing.

Reanalysis data. Six-hourly geopotential height and surface temperature data during 1970–2005 are used from the Japanese 55-year Reanalysis (JRA55)[31], which is one of very few datasets available before 1979.

Global aerosol–climate model simulations. The National Center for Atmospheric Research–Department of Energy CESM (version 1.2.2)—an updated version of CESM 1.0 participating in the Coupled Model Intercomparison Project Phase 5—is used in this study to simulate the historical variations of winter extreme weather and to conduct attribution analyses. The atmospheric circulation model (Community Atmosphere Model 5.4) fully interacts with an ocean circulation model (Parallel Ocean Program 2), a sea ice model (CICE) and a land-surface model (Community Land Model) through a central coupler. The model is configured with 1° horizontal resolution in both atmosphere and ocean models. Six types of aerosols (sulfate, black carbon, primary organic matter, secondary organic aerosol, sea salt and dust) are considered in the three-mode version of Modal Aerosol Module 3. The aerosol interactions with atmospheric radiation fluxes, aerosol–cloud interaction (grid-scale stratiform clouds) and the effect of absorbing aerosols (black carbon and dust) deposited in the snowpack are explicitly considered in the physics of CESM 1. More details regarding the treatments of aerosol, clouds and convection in CESM 1 can be found in our previous work[4,20].

To precisely assess the impacts of the anthropogenic emission shift, we confined our analysis period to 1970–2005, during which time the geospatial contrast of anthropogenic aerosol trends was the largest and occurred contemporaneously with greenhouse gas emissions. To minimize the spread of internal model variability from transient radiative forcing before 1970, one historical simulation was first created from 1850–1970, and then ensemble sensitivity simulations branched out for another 36-year integration. Two emissions scenarios were considered during 1970–2005: ALL and NO_AERO. Considering the significant nonlinearity in certain climate responses to different external forcings[32–34], such as the wave activity in the present study, the differences between those two experiments can only be interpreted as the qualitative importance of aerosol effects for those results. We prefer this method to aerosol-only simulations that ignore all other forcings and deviate from the real climate state. Accounting for the dependence of aerosol forcing on all other forcings is especially important in the transient forcing experiments that aim to mimic the real world. For the near-future radiative forcing changes, we conducted CESM simulations using the Representative Concentration Pathway 4.5 forcing scenario. Since the major reductions in the aerosol and precursor gas emissions will be achieved before 2050 (ref. [20]), our future trend analysis focuses on the period 2015–2045.

Data availability

The reanalysis products used in this study are publicly available from the NCAR Research Data Archive (https://rda.ucar.edu/datasets/ds628.0/). Monthly mean climate indices are available from the NOAA Climate Prediction Center (https://www.esrl.noaa.gov/psd/data/climateindices/list/).

Code availability

The code of the NCAR CESM model used in this study is available at http://www2.mmm.ucar.edu/wrf/users/download/get_source.html. The scripts used to process the model data can be found on the public website of corresponding author Y.W. (http://web.gps.caltech.edu/~yzw/share/Wang-2020-NCC).

References

29. Garfinkel, C. I. & Waugh, D. W. Tropospheric Rossby wave breaking and variability of the latitude of the eddy-driven jet. *J. Clim.* **27**, 7069–7085 (2014).
30. Smith, D. M. et al. Role of volcanic and anthropogenic aerosols in the recent global surface warming slowdown. *Nat. Clim. Change* **6**, 936–940 (2016).
31. Harada, Y. et al. The JRA-55 reanalysis: representation of atmospheric circulation and climate variability. *J. Meteorol. Soc. Jpn* **94**, 269–302 (2016).
32. Feichter, J., Roeckner, E., Lohmann, U. & Liepert., B. Nonlinear aspects of the climate response to greenhouse gas and aerosol forcing. *J. Clim.* **17**, 2384–2398 (2004).
33. Ming, Y. & Ramaswamy, V. Nonlinear climate and hydrological responses to aerosol effects. *J. Clim.* **22**, 1329–1339 (2009).
34. Ming, Y., Ramaswamy, V. & Chen, G. A model investigation of aerosol-induced changes in boreal winter extratropical circulation. *J. Clim.* **24**, 6077–6091 (2011).

Acknowledgements

This study is supported by the NASA ROSES ACMAP and CCST, and NSF grants AGS-1700727 and AGS-1742178. We acknowledge the support of the Jet Propulsion Laboratory, California Institute of Technology, under contract with NASA. We also acknowledge high-performance computing support from Pleiades, provided at NASA Ames. The CESM project is supported primarily by the National Science Foundation. All correspondence and requests for materials should be addressed to Y.W. (yuan.wang@caltech.edu).

Author contributions

Y.W. and J.H.J. designed the research. Y.W. obtained the data and performed the model simulations. T.L., Y.W., G.C. and Y.L.Y. analysed the data. Y.W. wrote the paper. J.H.S., G.C., Y.L.Y., H.S., J.H.J. and T.L. commented on and edited the paper.

Competing interests

The authors declare no competing interests.

Additional information

Supplementary information is available for this paper at https://doi.org/10.1038/s41558-020-0693-4.

Correspondence and requests for materials should be addressed to Y.W. or J.H.J.

Peer review information *Nature Climate Change* thanks Marie McGraw, Zhaoyi Shen and the other, anonymous, reviewer(s) for their contribution to the peer review of this work.